

Ault et al., 2016, Lithosphere Data Repository

ANALYTICAL METHODS

Hematite texture scanning electron microscopy

Secondary electron (SE) images of representative hematite aliquots from each sample were acquired on a Quanta 650 FEG scanning electron microscope at Utah State University's Microscopy Core Facility. Aliquots used for (U-Th)/He analysis are consumed during the measurement process. Therefore, representative aliquots from Gower, Glamorgan, and Cumbria hematite samples were prepared for SE imaging in two ways. Gower aliquots were affixed to a sample holder using conductive copper sticky tape and Glamorgan and Cumbria aliquots were mounted in epoxy in a 1" plastic ring form, polished, and carbon-coated. SE imaging of all aliquots occurred in low vacuum-variable pressure mode at 0.5-0.8 Torr, with 16-20 kV accelerating voltage, 65 nA current, and 8.5-11.4 mm working distance. Images were acquired at various scales such that images at the smallest field of view are a component of the larger field of view. Images are annotated to show these relationships and the self-similarity of the grain size distribution in each aliquot (Fig. DR3). SE images taken at 100000x-200000x for Gower samples Lsl-1, Lsl-6, EOx-8, and WCB-1; 50000x for Cumbria sample A14-1; and 5000x Glamorgan sample LLW-2 were used for grain size measurements. The thickness (diameter) of 5-13 individual plates was measured for each sample using the SEM's distance line tool. Minimum and maximum plate radii (half-width) are reported in Table DR1.

(U-Th)/He methods

He degassing and U-Th analyses of hematite and apatite were conducted at the University of Arizona Radiogenic Helium Dating Laboratory (ARHDL).

Hematite: Chips of hematite ~1-2 mm in diameter were extracted the fault surfaces using fine point tweezers and a dremel tool. These chips were then broken into replicate aliquots. Aliquots of hematite were selected to avoid dremel tool marks and boundaries with other phases. Aliquots were thus selected from the interior of the hematite material, greater than one α -stopping distance (i.e., >20 μ m) away from the hematite-host rock interface, so an α -ejection correction factor is not applied to the He dates. Individual aliquots were loaded into Nb packets. Hematite

aliquots were heated to temperatures and packet “glow” comparable to apatite for ~8-10 minutes using a diode laser in an ultra-high vacuum gas extraction line. Extracted He gas was spiked with ^3He , purified using cryogenic and gettering methods, and analyzed on a quadrupole mass spectrometer. Each aliquot was heated a second time to temperatures slightly greater than the first extraction but negligible gas was released. Analysis of a known quantity of ^4He was performed after every 4-5 unknown analyses to monitor instrumental sensitivity drift. U and Th contents of each aliquot were measured by isotope dilution and solution ICPMS, as described by Reiners (2005). Prior analyses in the ARHDL indicate that hematite does not fully dissolve in nitric acid, hydrochloric acid, or aqua regia, requiring HF dissolution in a pressure digestion vessel (Parr bomb). Following addition of a ^{233}U - ^{229}Th spike, equilibration, and dissolution, U and Th isotopes were measured on an Element 2 ICP-MS. Fish Canyon Tuff zircon was used as a standard and analyzed by the same procedures with the batch of unknowns. No alpha-ejection corrections are required for the hematite He dates because the aliquots are part of a larger initial sample with dimensions larger than the alpha-stopping distance. Hematite dates were determined assuming that the grains were unzoned in U and Th. Samples do not exhibit a correlation between individual date and Th/U ratio (Fig. DR5), supporting that U volatilization and loss did not occur during lasing (Vasconcelos et al., 2013).

Apatite: Single crystals of apatite were selected based on morphology, clarity, and lack of inclusions using a binocular microscope with crossed polars. Individual apatites were imaged, length and width dimensions measured on two sides, and loaded into Nb packets. Apatites were laser heated to ~1065 °C for three minutes with a diode laser without a gas re-extract. Extracted He gas was spiked with ^3He , purified using cryogenic and gettering methods, and analyzed on a quadrupole mass spectrometer. The degassed apatites were retrieved, spiked with a ^{233}U - ^{229}Th - ^{147}Nd - ^{42}Ca tracer, dissolved in HNO_3 at ~90 °C for 1 hour, and analyzed on an Element 2 ICP-MS. The apatite mass was computed as the dimensional mass from the apatite radius and length measurements. This dimensional mass was used to calculate the apatite U, Th, and Sm concentrations. Fragments of the Durango apatite were used as a standard. A hexagonal prism morphology was used as a reasonable approximation for the apatite alpha-ejection correction (Farley et al., 1996) and apatites are assumed to be unzoned in U, Th, and Sm.

Zircon: Single crystals of zircon were selected based on morphology and clarity, and minimal inclusions when possible using a binocular microscope with crossed polars. Individual zircons were imaged, length, width, and tip heights dimensions measured on two sides, and loaded into Nb packets. Zircons were laser heated to ~1250 °C for 15 minutes followed by 1-2 gas re-extracts at higher temperatures to purge the grains of He using a diode laser on an ultra-high vacuum gas extraction line. Extracted He gas was spiked with ^3He , purified using cryogenic and gettering methods, and analyzed on a quadrupole mass spectrometer. Analysis of a known quantity of ^4He was performed after every 4-5 unknown analyses to monitor instrumental sensitivity drift. Following addition of a ^{233}U - ^{229}Th spike, equilibration, and dissolution in HF in dissolution in a Parr bomb, the U and Th isotopes were measured on an Element 2 ICP-MS. Fish Canyon Tuff zircon was used as a standard and analyzed by the same procedures with the batch of unknowns. The alpha ejection correction of Hourigan et al. (2005) was used.

Apatite fission-track methods

Apatite grains were mounted in epoxy resin, alumina and diamond polished, and spontaneous fission tracks revealed by etching with 5.5M HNO_3 at 20°C for 20 seconds. Samples were analyzed by applying the external detector method (Gleadow, 1981) using very low uranium, annealed muscovite mica detectors, and irradiated at the Oregon State University Triga Reactor, Corvallis, USA. The neutron fluence was monitored using European Institute for Reference Materials and Measurements (IRMM) uranium-dosed glasses IRMM 540R. After irradiation, induced tracks in the mica external detectors were revealed by etching with 48% HF for 18 minutes. Spontaneous and induced FT densities were counted using an Olympus BX61 microscope at 1250x magnification with automated Kinetek Stage system. Apatite FT lengths and Dpar values were measured using an attached drawing tube and digitizing tablet supplied by Trevor Dumitru of Stanford University calibrated against a stage micrometer. Central ages (Galbraith and Laslett, 1993), quoted with 1σ errors, were calculated using the IUGS recommended Zeta-calibration approach of Hurford and Green (1983). An apatite IRMM 540R zeta calibration factor of 368.1 ± 14.9 was obtained by repeated calibration against a number of internationally agreed age standards including Durango and Fish Canyon apatite according to the recommendations of Hurford (1990).

REFERENCES

- Farley, K.A., Wolf, L.T., and Silver, L.T., 1996, The effects of long alpha-stopping distances on (U-Th)/He ages. *Geochimica et Cosmochimica Acta* **60**, 4223-4229.
- Galbraith, R.F., and Laslett, G.M., 1993, Statistical models for mixed fission track ages. *Nuclear Tracks* **21**, 459-470.
- Gleadow, A.J.W., 1981, Fission-track dating methods: what are the real alternatives? *Nuclear Tracks* **5**, 3-14.
- Hourigan, J.K., Reiners, P.W., and Brandon, M.T., 2005, U-Th zonation-dependent alpha-ejection in (U-Th)/He chronometry. *Geochimica et Cosmochimica Acta* **69**, 3349-3365.
- Hurford, A.J., 1990, Standardization of fission track dating calibration: Recommended by the Fission Track Working Group of the I.U.G.S. Subcommittee on Geochronology. *Chemical Geology* **80**, 171-178.
- Hurford, A.J., and Green, P.F., 1983, The zeta-age calibration of fission-track dating. *Isotope Geoscience* **1**, 285-317.
- Reiners, P.W., 2005, Zircon (U-Th)/He thermochronometry. *Reviews in Mineralogy and Geochemistry* **58**, 151-179.
- Vasconcelos, P.M., Heim, J.A., Farley, K.A., Monteiro, H., and Waltenberg, K., 2013, $^{40}\text{Ar}/^{39}\text{Ar}$ and (U-Th)/He - $^4\text{He}/^3\text{He}$ geochronology of landscape evolution and channel iron deposits genesis at Lynn Peak, Western Australia. *Geochimica et Cosmochimica Acta* **117**, 283-312.

Table DR1. Estimated hematite (U-Th)/He closure temperatures.

Sample	a^a (μm) min	a (μm) max	Tcl^b (°C) min	Tcl (°C) max
Lsl1	0.075	0.175	82	94
Lsl6	0.05	0.2	77	96
EOx8	0.03	0.04	70	74
WCB1	0.025	0.05	68	77
LLW2	0.5	5	110	150
A14-11	0.03	0.04	70	74

^a Diffusion domain length-scale is plate half-width measured from SEM SE images.

^b Closure temperatures calculated assuming $E_a = 147.5$ kJ/mol and $D_0 = 2.2E-4$ cm²/s (Evenson et al., 2014), spherical geometry, and 10 °C/Myr cooling rate

Table DR2. Hematite (U-Th)/He data from Gower Peninsula, Glamorgan Peninsula, and Cumbria

	U (ng)	± 1σ	Th (ng)	± 1σ	Th/U	He (pmol)	± 1σ	Date (Ma)	Error (Ma) ^a
Gower Peninsula, Wales									
<i>Lsl-1: Limeslade</i>									
H1	3.263	0.049	0.004	0.000	0.001	2.030	0.015	114.26	1.88
H2	3.375	0.051	0.005	0.000	0.002	2.199	0.018	119.61	2.02
H3	2.959	0.047	0.005	0.000	0.002	2.041	0.015	126.53	2.17
H4	4.013	0.061	0.007	0.000	0.002	2.605	0.021	119.17	2.02
								119.9 ± 5.0 Ma^b	
								<i>MSWD</i> ^c = 6.2	
<i>Lsl-6: Limeslade</i>									
H1	2.117	0.033	0.006	0.000	0.003	1.598	0.010	138.25	2.27
H2	1.777	0.027	0.006	0.000	0.003	1.234	0.009	127.32	2.12
H3	1.830	0.027	0.005	0.000	0.003	1.489	0.010	148.92	2.39
H4	1.983	0.032	0.006	0.000	0.003	1.533	0.010	141.60	2.45
H5	0.812	0.012	0.004	0.000	0.005	0.641	0.005	144.45	2.40
								140.1 ± 8.1 Ma	
								<i>MSWD</i> = 13.6	
<i>WCB-1: Fox Hole/Westcliff Bay</i>									
H1	5.801	0.091	0.036	0.001	0.006	4.659	0.072	146.90	3.20
H2	3.546	0.055	0.051	0.001	0.015	2.672	0.040	137.68	2.95
H3	0.930	0.014	0.017	0.000	0.019	0.692	0.010	135.88	2.86
H\$	1.747	0.028	0.021	0.000	0.012	1.374	0.021	143.65	3.16
								141.0 ± 5.1 Ma	
								<i>MSWD</i> = 2.9	
<i>Eox-8: Oxwich Fault East</i>									
H1	5.769	0.089	0.024	0.000	0.004	4.109	0.064	130.52	2.84
H3	2.871	0.044	0.007	0.000	0.002	2.161	0.033	137.89	2.96
								134.2 ± 5.2 Ma	
								<i>MSWD</i> = 3.2	
Glamorgan Peninsula, Wales									
<i>LLW2: Llanharry</i>									
H1	0.751	0.011	0.004	0.000	0.006	0.453	0.002	110.71	1.64
H2	1.359	0.019	0.007	0.000	0.005	0.690	0.003	93.33	1.37
H3	0.766	0.011	0.014	0.000	0.019	0.338	0.002	81.00	1.20
H4	0.916	0.013	0.006	0.000	0.007	0.486	0.002	97.39	1.42
H5	1.094	0.016	0.005	0.000	0.005	0.608	0.003	102.04	1.52
H6	1.237	0.018	0.004	0.000	0.003	0.661	0.003	98.21	1.43
								97.1 ± 9.8 Ma	
								<i>MSWD</i> = 66.8	
Cumbria - Lake District, England									
<i>A14-11: Cumbria botryoidal</i>									
H1	0.273	0.004	0.001	0.000	0.005	0.176	0.001	118.25	1.82
H2	0.372	0.006	0.001	0.000	0.003	0.236	0.001	116.37	1.83
H3	0.209	0.003	0.001	0.000	0.005	0.134	0.001	117.29	1.75
H4	0.337	0.005	0.001	0.000	0.003	0.214	0.001	116.66	1.77
H5	0.184	0.003	0.001	0.000	0.004	0.119	0.001	118.59	1.83
								117.4 ± 1.0 Ma	
								<i>MSWD</i> = 0.3	

^a ± 1σ error propagated from analytical uncertainties on the U, Th, and He measurements

^b Sample mean and 1σ standard deviation of the mean

^c MSWD, mean square of weighted deviates, calculated as
$$MSWD = \frac{1}{n-1} \sum_{i=1}^n \frac{(t_i - \bar{t})^2}{\sigma_i^2}$$
 where σ_i is the reported individual 1σ error

Table DR3. Apatite and zircon (U-Th)/He data from sedimentary infill sample OX-1 (51.544739°N, -4.165461°E)

	mass ^a (μg)	r ^b (μm)	l ^c (μm)	U (ppm)	Th (ppm)	eU (ppm)	Sm (ppm)	⁴ He (nmol/g)	Ft ^d	Raw date (Ma)	Corr date (Ma)	Error ^e (Ma)
APATITE												
a1	0.00008	33.25	112.50	19.04	37.17	27.78	27.39	3.97	0.59	26.4	44.8	0.8
a2	0.00006	32.50	95.00	26.87	90.08	48.04	179.35	7.90	0.56	30.2	53.6	1.2
a3	0.00005	24.00	115.50	26.36	96.47	49.03	361.18	7.36	0.48	27.5	57.2	1.1
a4	0.00012	37.00	125.00	26.46	39.70	35.79	126.76	7.45	0.63	38.3	61.0	1.2
a5	0.00004	24.75	108.00	28.45	145.40	62.62	194.88	29.69	0.48	86.8	180.1	2.6
a6	0.00004	22.50	95.00	52.33	136.05	84.31	156.85	10.05	0.44	22.0	49.3	0.9
a7	0.00004	22.75	108.50	43.90	91.35	65.37	271.92	7.47	0.46	21.0	45.4	1.0
a8	0.00003	25.50	138.00	37.10	70.44	53.65	180.27	6.15	0.52	21.1	40.7	0.9
ZIRCON												
z1	0.0009	25.0	170.5	367.46	154.63	403.80	-	579.57	0.65	260.2	401.5	8.1
z2	0.0006	19.8	133.0	373.59	113.33	400.23	-	360.85	0.56	164.9	291.8	4.4
z3	0.0007	27.3	119.0	263.73	222.97	316.13	-	360.79	0.65	207.9	320.2	4.6
z4	0.0012	27.5	141.5	108.37	107.88	133.72	-	155.26	0.66	211.5	323.1	4.4
z5	0.0008	27.5	114.0	313.91	254.99	373.83	-	371.78	0.65	181.6	282.8	4.0
z6	0.0004	19.0	102.5	105.83	137.19	138.07	-	115.89	0.54	153.6	292.2	4.2
z7	0.0006	23.5	133.5	483.35	193.95	528.93	-	459.48	0.61	158.9	259.5	3.8
z8	0.0012	28.3	155.5	514.83	120.17	543.07	-	578.19	0.66	194.2	292.3	4.5

^a Ca-based mass for apatite and Zr-based mass for zircon

^b Average radius

^c Average length

^d Ft - alpha ejection correction of Farley et al, (1996) for apatite and Hourigan et al. (2005) for zircon

^e 1σ analytical uncertainty propagated from the U, Th, and He measurements and grain length uncertainties

Table DR4. Apatite fission-track data from sedimentary infill sample Ox-1

Sample No.	No. of Crystals	Track Density (x 10 ⁶ tr cm ⁻²)			$\rho_s/\rho_i \pm 1\sigma$	Mean Dpar (μm)	Age Dispersion (P χ^2)	Central Age $\pm 1\sigma$ (Ma)
		ρ_s (N _s)	ρ_i (N _i)	ρ_d (N _d)				
OX-1	7	1.806 (89)	2.009 (99)	0.8028 (2569)	0.8990±0.1374	2.21	<0.01% (99.8%)	131.4±20.1

Notes:

- (i). Analyses by external detector method using 0.5 for the $4\pi/2\pi$ geometry correction factor;
- (ii). Ages calculated using dosimeter glass: IRMM540R with $\zeta_{540R} = 368.1 \pm 14.9$ (apatite);
- (iii). P χ^2 is the probability of obtaining a χ^2 value for v degrees of freedom where v = no. of crystals - 1;

Sample Number **OX-1**
 Position (#) 40
 Area of Graticule Square 6.400E-07
 No. of Crystals 7
 Zeta Factor ± Error 368.1 14.9
 Rho d (% Relative Error) 8.028E+05 1.97
 N d 2569

Mineral **Apatite**
 Glass (U pp) 15
 Irradiation UA-A17
 Analyst SNT
 Count Date 1.5.2014
 Locality
 Rock Type

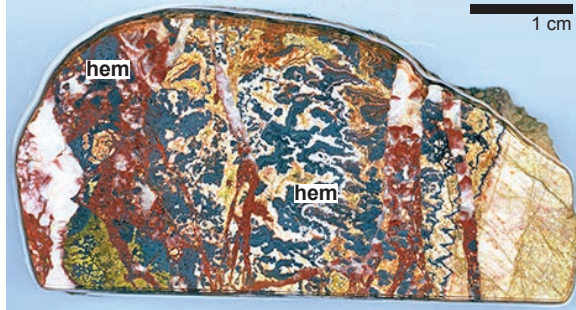
N s	N i	N g	Dpar	Dper	Rmr0	p s	p i	p s / p i	U ppm	Age (Ma)	Age error	50% Age	" +95% "	" -95% "
10	10	9	1.86	0.53	0.824	1.736E+06	1.736E+06	1.0000	32.4	146.09	65.66	161.01	222.88	106.05
6	8	8	2.32	0.54	0.793	1.172E+06	1.563E+06	0.7500	29.2	109.87	59.55	127.23	227.05	95.62
13	16	12	2.12	0.42	0.807	1.693E+06	2.083E+06	0.8125	38.9	118.95	44.74	127.62	133.22	74.72
21	22	12	2.17	0.53	0.803	2.734E+06	2.865E+06	0.9545	53.5	139.52	43.03	146.09	117.33	72.72
3	3	12	3.01	1.20	0.734	3.906E+05	3.906E+05	1.0000	7.3	146.09	119.46	199.74	818.58	179.98
23	27	9	1.94	0.48	0.819	3.993E+06	4.688E+06	0.8519	87.6	124.65	35.81	129.82	94.22	61.24
13	13	15	2.02	0.52	0.814	1.354E+06	1.354E+06	1.0000	25.3	146.09	57.68	157.48	179.52	94.68
*****	*****	*****	*****	*****	*****	*****	*****	*****	*****	*****	*****	*****	*****	*****
89	99	77	2.21	0.60	0.799	1.806E+06	2.009E+06	0.8990	37.5	131.48	20.10	132.90	43.35	35.02
Pooled Ratio			0.8990	±	0.1374									
Mean Ratio			0.9098	±	0.0393									
Pooled Age			131.48	±	20.10	1 S.E.								
Mean Crystal Age			133.05	±	5.80	1 S.E.								
Binomial Age			132.90	+	43.35	" +95% "								
				-	35.02	" -95% "								

Central Age **131.48 ± 20.10**

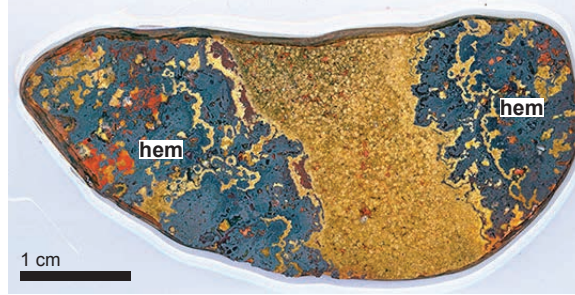
Age Dispersion **0.00 %**
Chi-squared **0.409** with 6 degrees of freedom
P (Chi-Sq) **99.88 %**

Gower Peninsula samples

Ls11



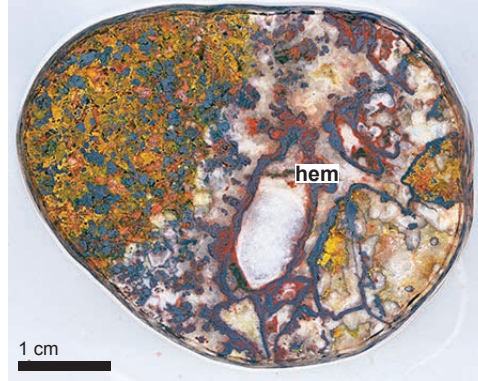
Ls16



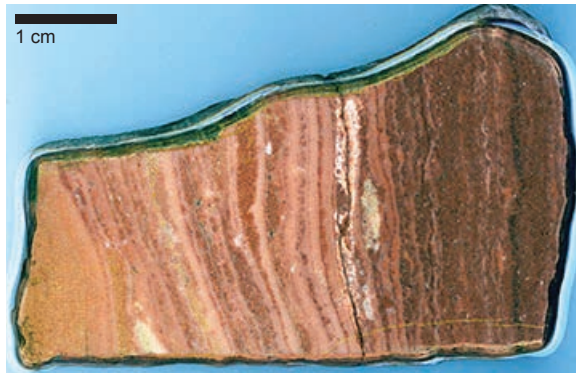
WCB1



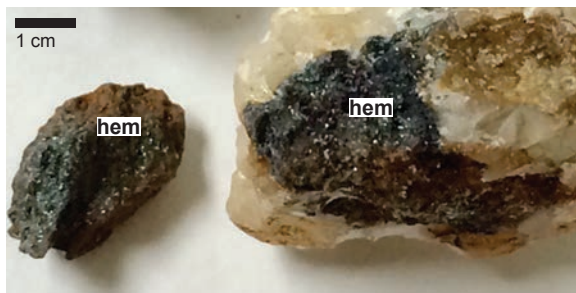
EOx8



Ox1 - sandstone infill



Glamorgan Peninsula sample LLW2



Cumbria sample A14-11



Figure DR1. Hand sample photographs of portions of Gower fissure fill, Glamorgan, and Cumbria samples. Hem = hematite.

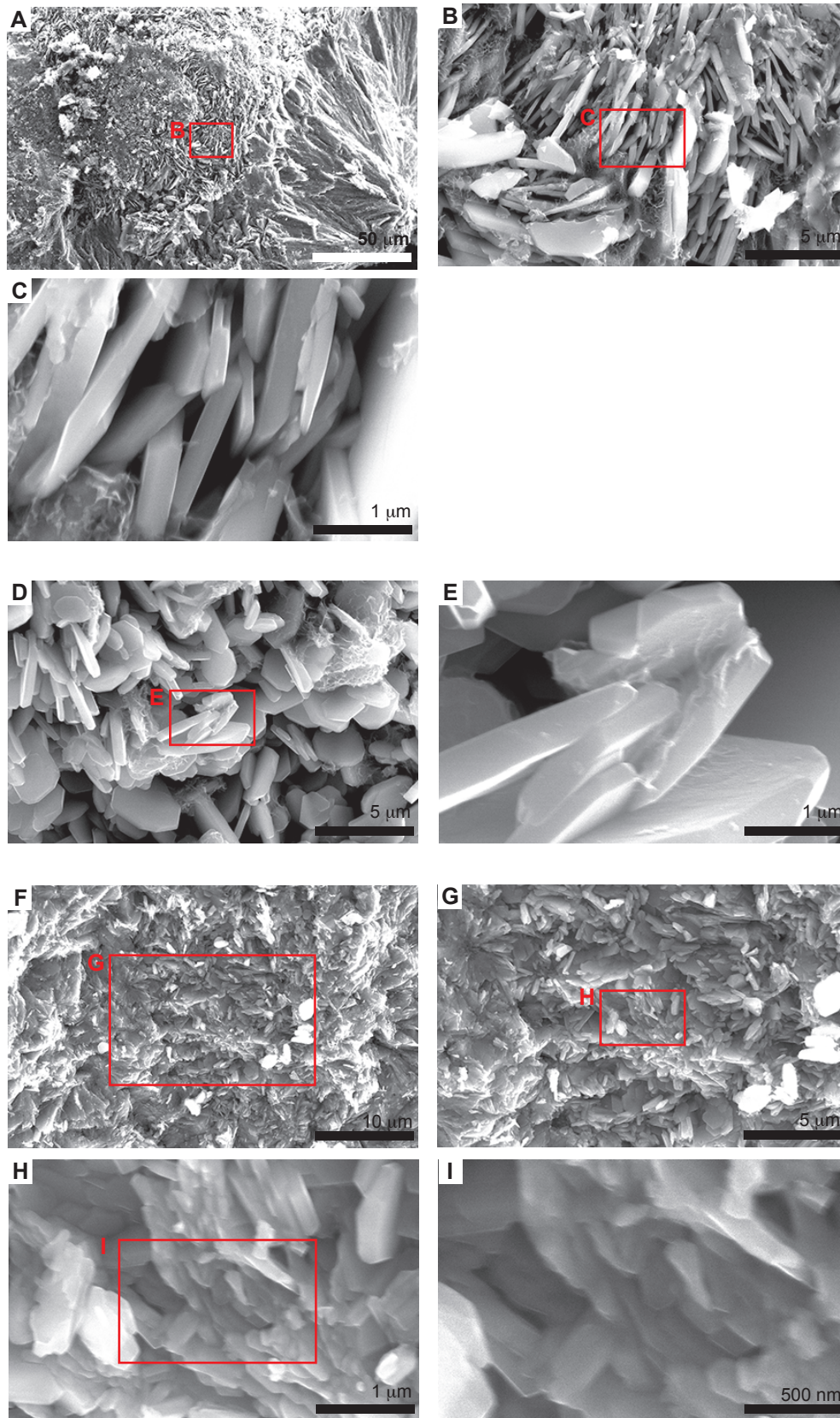


Figure DR2. SEM SE images taken at different scales from representative hematite aliquots of Gower sample Ls11.

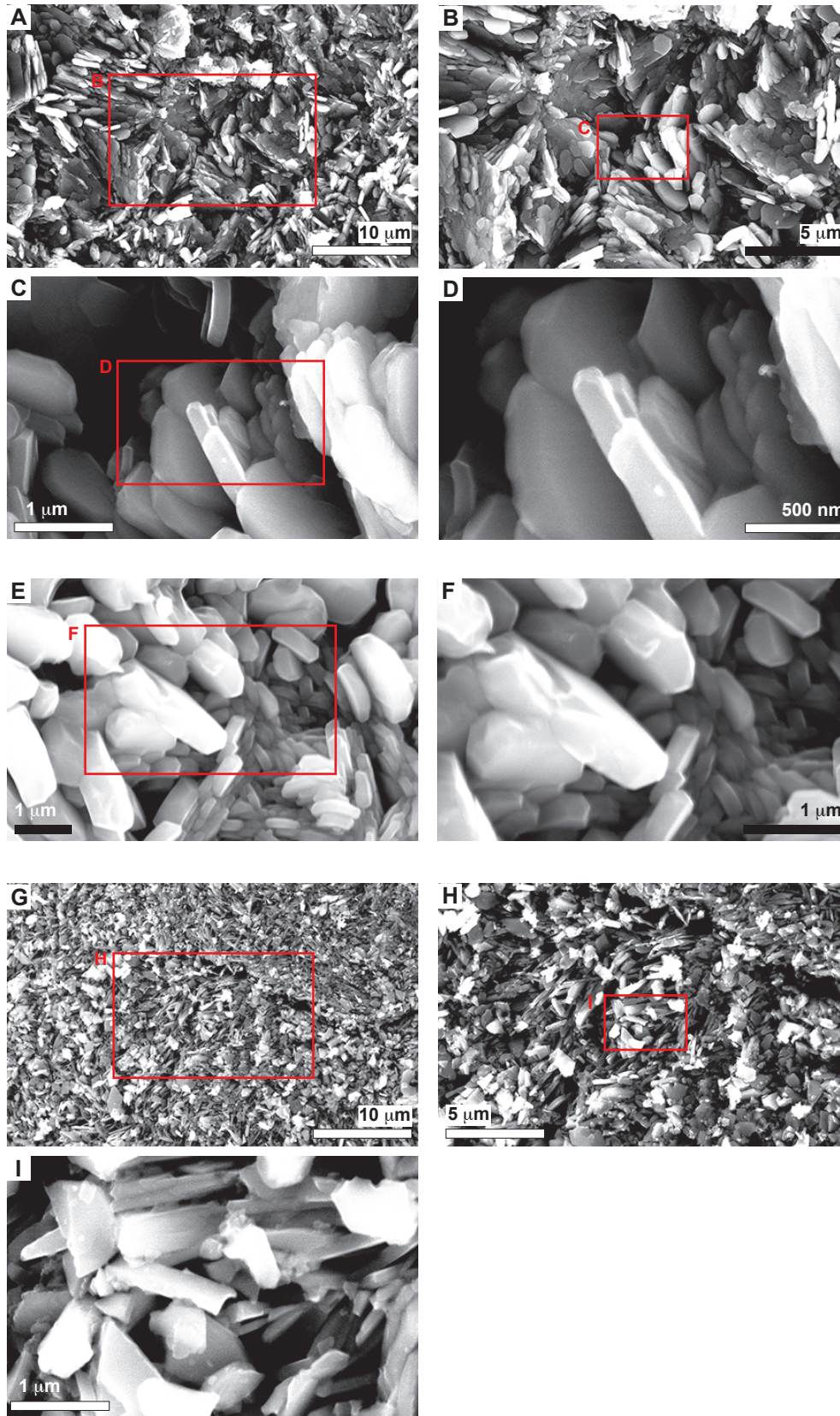


Figure DR2 continued. SEM SE images taken at different scales from representative hematite aliquots of Gower sample Lsl6.

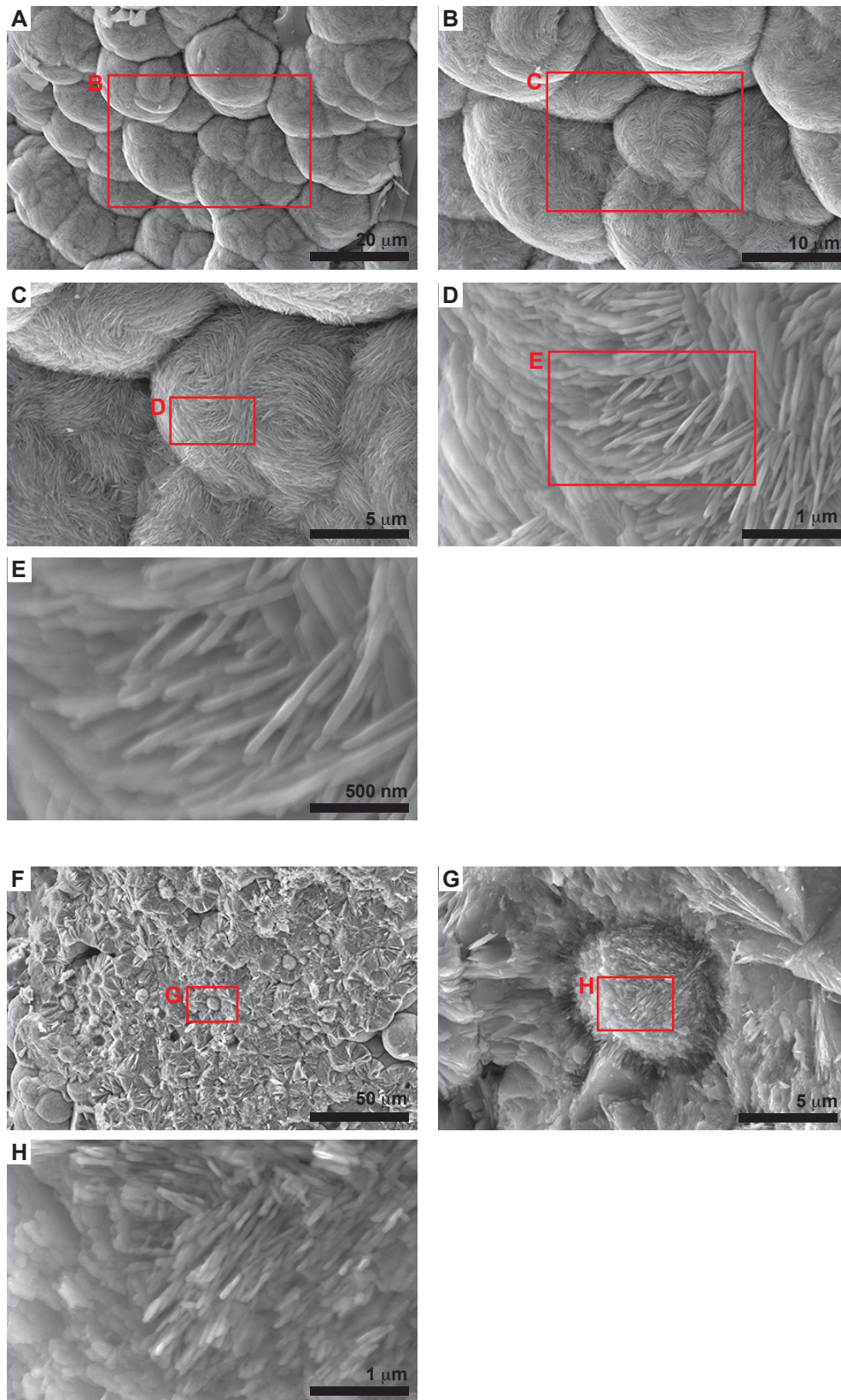


Figure DR2 continued. SEM SE images taken at different scales from representative hematite aliquots of Gower sample EOx8.

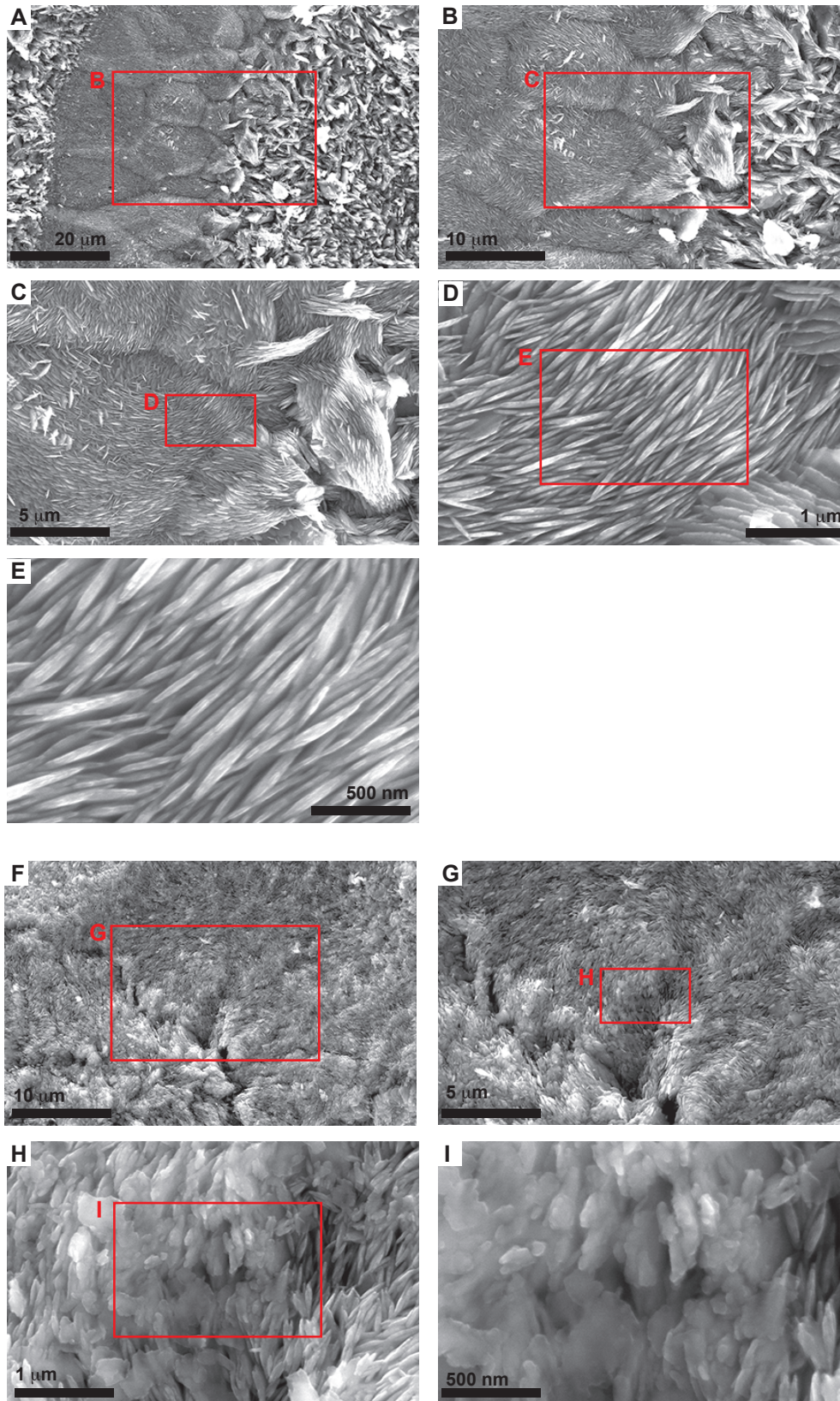


Figure DR2 continued. SEM SE images taken at different scales from representative hematite aliquots of Gower sample WCB1.

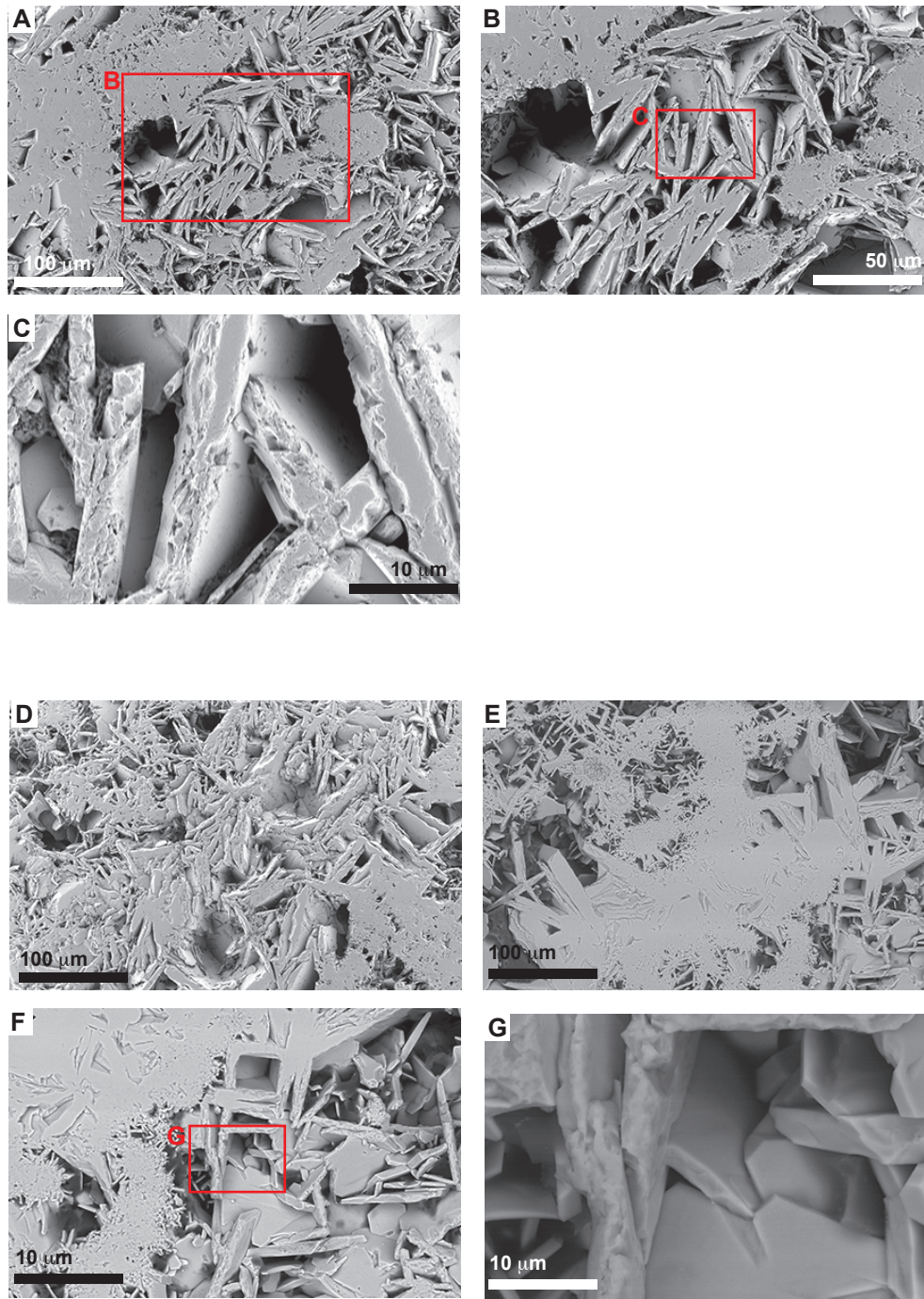


Figure DR2 continued. SEM SE images taken at different scales from representative hematite aliquots from Glamorgan sample LLW2.

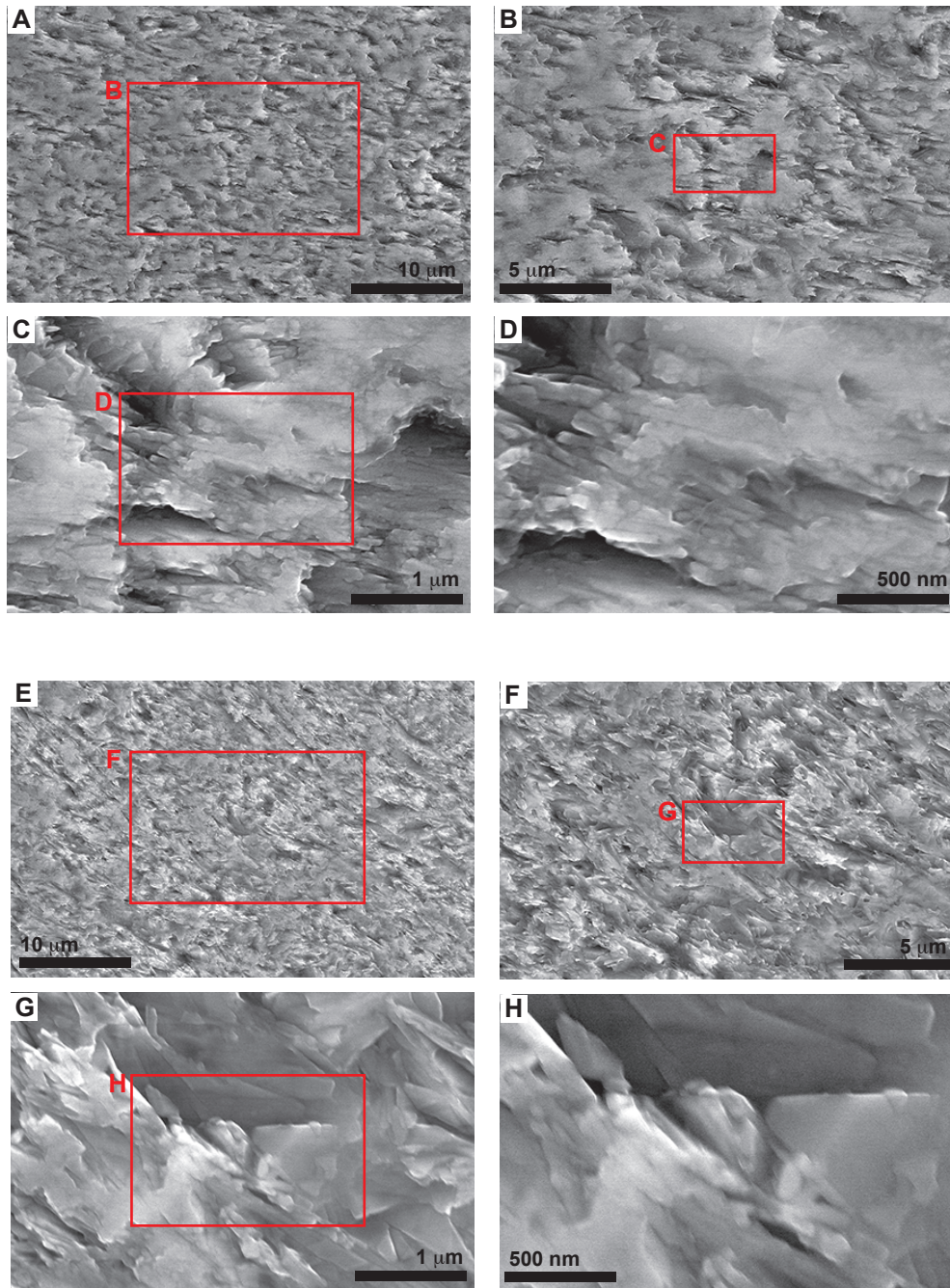
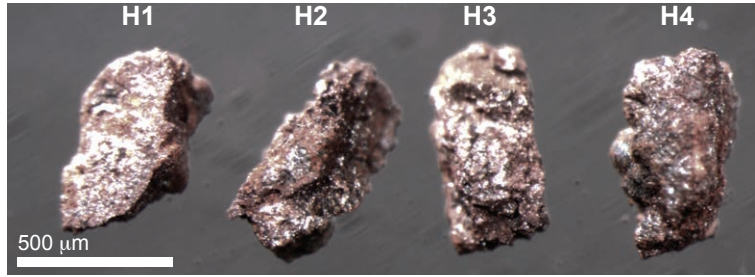
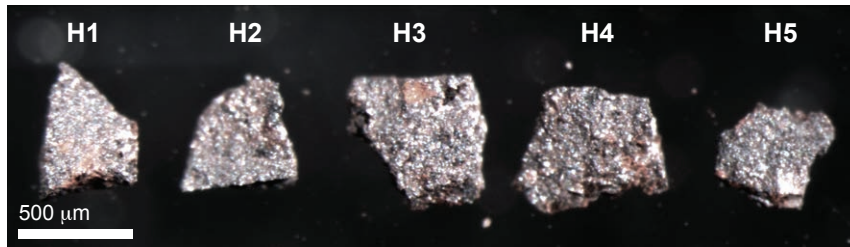


Figure DR2 continued. SEM SE images taken at different scales from representative hematite aliquots of Cumbria sample A14-11.

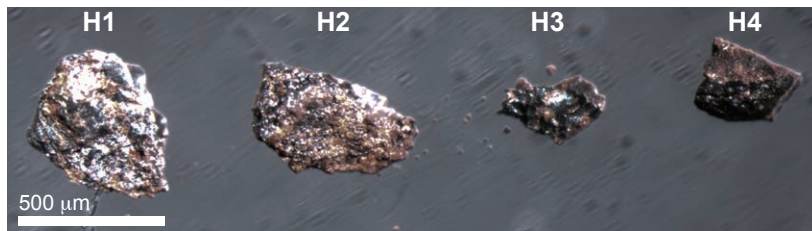
Lsl-1



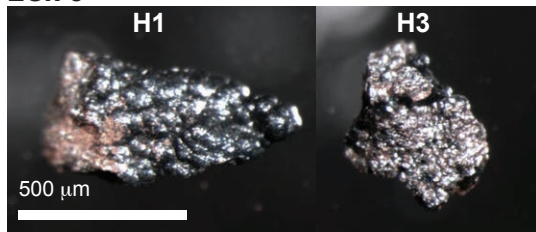
Lsl-6



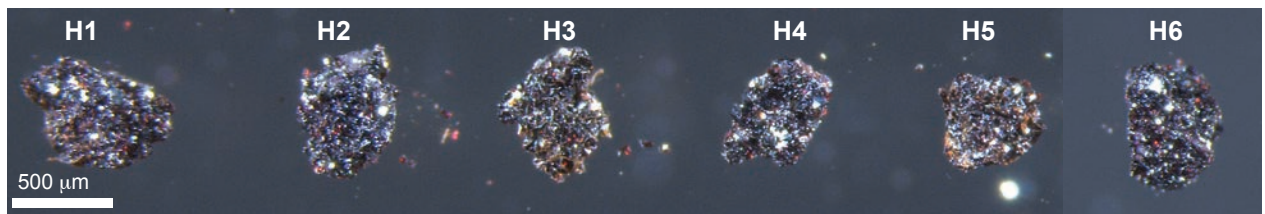
WCB-1



EOx-8



LLW2



A14-11

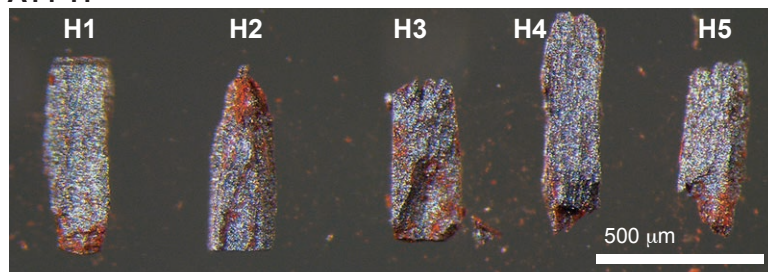


Figure DR3. Photographs of hematite aliquots analyzed for (U-Th)/He dating from the Gower, Glamorgan, and Cumbria samples.

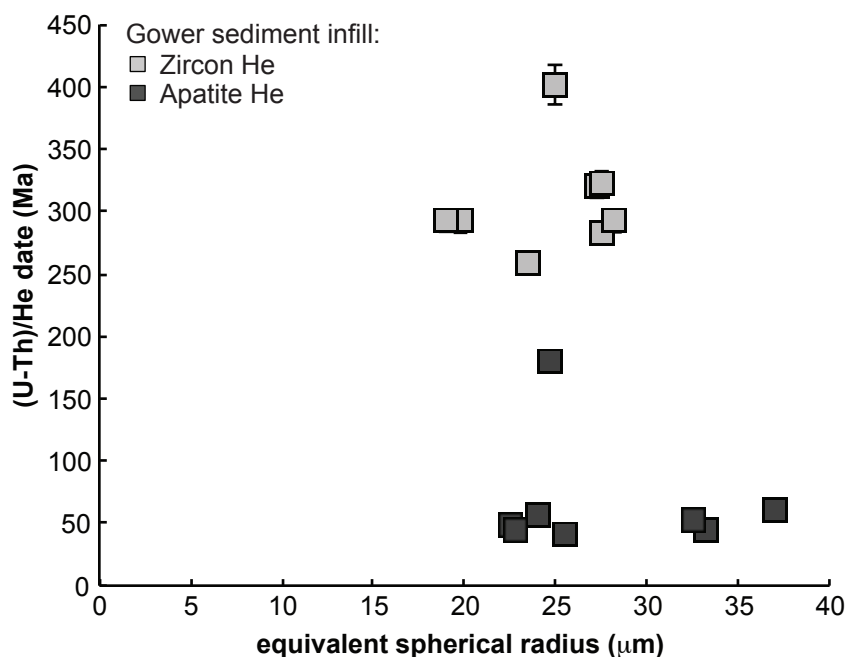


Figure DR4. Individual zircon and apatite (U-Th)/He dates from sedimentary infill sample Ox-1 as a function of equivalent spherical radius. Individual date errors plotted as the 2σ analytical uncertainty.

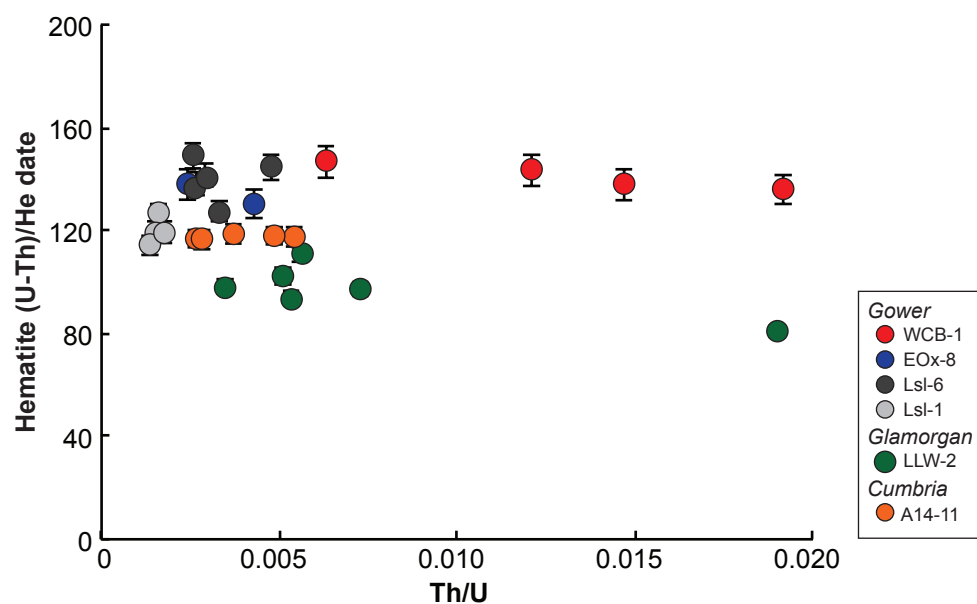


Figure DR5. Individual hematite (U-Th)/He date as a function of Th/U ratio. Data classified according to sample. Individual date errors plotted as the 2σ analytical uncertainty.